Velocity Fields with Power-Law Spectra for Modeling Turbulent Flows

Mine Çağlar

Koç University

Istanbul Turkey

mcaglar@ku.edu.tr

Abstract

We consider a generalization of homogeneous and isotropic Çinlar velocity fields to capture power-law spectra. The random velocity field is non-Gaussian with a representation motivated by Lagrangian and Eulerian observations. A wide range of turbulent flows can be generated by varying the stochastic parameters of the model. The velocity field being a functional version of Poisson shot-noise is constructed as the superposition of eddies randomized through their types and arrival times. We introduce a dependence between the eddy types which are spatial parameters and the decay parameter which is temporal. As a result, long-range correlation in space and a power-law spectrum previously used with Ornstein-Uhlenbeck velocity fields are achieved. We show that a corresponding power-law form for the probability distribution of the eddy diameter is sufficient for this result. The parameters of the probability distribution are further specified in view of Kolmogorov theory of the inertial scales. In particular, $|k|^{-5/3}$ scaling of the spectrum is obtained. In the diffusive limit, we show that the parameters governing the decay and the arrival rate, and the speed of rotation of an eddy increase while its diameter decreases. That is, the eddies arrive fast, decay fast, and rotate fast with a small radius for a Brownian limit.

Key Words: Stochastic flows; Kolmogorov spectrum; Hurst exponent; homogeneous turbulence.

1 Introduction

Lagrangian data collected from the ocean over the last two decades indicate that the flow in the ocean is much more correlated than a random walk or a Brownian flow. Significant research efforts have gone to model the Eulerian velocity field or the Lagrangian motion to capture such correlations. In particular, the class of velocity fields introduced by Çinlar [1, 2] is motivated by small to medium scale eddies. They can generate a wide range of flows as well as the features of stationary and homogeneous turbulence [3, 4, 5]. Our aim is to study a generalization of Çinlar flows that yield power-law spectra in view of Kolmogorov theory of the inertial scales. We provide a structural description in space and time domain for this purpose.

The velocity field being the functional version of Poisson shot-noise is constructed as the superposition of deterministic velocity fields. These are typically eddies randomized through their types and arrival times and decaying exponentially in time to form a stationary, Markov velocity field. The motivation comes from vortex development and decay observed in the ocean [6]. The eddies that comprise the isotropic velocity field are similar to those used in the vortex method, which is a numerical approach. In contrast to Brownian flows where the particle motions are diffusions and the Eulerian velocity is delta-correlated, Çinlar velocity field itself is Markovian resulting in medium to long-term correlated flows.

In this paper, we introduce a generalization to Çinlar velocity field such that stationarity still holds, but with a power-law correlation across scales. This is achieved by making the decay rate depend on the spatial parameters determined by the type of an eddy. The resulting velocity field is no more Markovian, but captures the power-law spectra assumed by physical considerations. More explicitly, the velocity field and its flow statistics depend essentially on two parameters δ and γ. The parameter δ which is involved in the eddy diameter distribution governs the spatial correlation in the inertial range, and γ which goes into the decay rate expression controls the temporal correlation in Kolmogorov spectrum. We show that the slope of the wave spectrum in this case is $\delta - 3$, which can be made equal to -5/3 with the choice $\delta = 4/3$. That is, the energy spectrum $\mathcal{E}(|k|)$ can be made proportional to $|k|^{-5/3}$ when $|k|$ takes values in the inertial range $(1/l_2, 1/l_1)$ where $l_1, l_2 \in \mathbb{R}$ are the corresponding length scales. We also consider the range $(0, 1/l_2)$ where a parameter θ serves as the counterpart of δ. The parameter θ must assume values greater than 2 for finite energy and long-range correlation in space occurs when $2 < \theta < 3$. The rigorous formulations of all these are carried out based on the probability distribution of the eddy diameter. As for temporal correlations, the case $\gamma = 0$ reduces to the original Çinlar model and we have a Markovian velocity field taking values in $C(\mathbb{R}^d \to \mathbb{R}^d)$. For $\gamma > 0$, the temporal correlation depends on the spatial scales and we show that $\gamma = 1/3$ is indicated by Kolmogorov scaling.

Kolmogorov 5/3 law can also be replicated with assumptions only on the probability distributions of the original Çinlar velocity field where the decay rate in time is a constant [8]. On the other hand, as the temporal correlation is related to the spatial scales in the present study, both long-lived structures in time and power-law scaling in space are achieved. The resulting power-law spectra is similar to those used in earlier models [9, 10] where Ornstein-Uhlenbeck flows form a particular Gaussian and Markovian case. Some others [11] include shear flows in particular. Such models are constructed with assumptions on the spectra, whereas our model originates from observed structures of eddies and randomness in the ocean. We obtain the spectral properties as a consequence of the choice of the parameters and the probability distributions.

We prove the diffusive limit for $\gamma = 0$ by scaling the time through fast arriving, but short-lived eddies in addition to a scaling in space. Since our tools rely on Markov property, these results are valid only for the Markovian version of the velocity field. The limit is related to model parameters specifically. The decay and the arrival rate, and the speed of rotation of an eddy increase while its diameter decreases. That is, the eddies arrive fast, decay fast, and rotate fast with a small radius for the single particle path to be approximated by a Brownian motion.

The velocity field model has sufficiently many parameters for exploiting eddy structures in a robust fashion. Recent high-frequency radar measurements of the ocean [6] have detected eddies of radii 1-5 km, which occur sporadically in time and space. The parameters of the original Çinlar velocity model have been estimated from these measurements in [7] which thus validates its applicability. Similarly, the stochastic velocity model of the present paper can potentially resolve such submesoscale eddies within more comprehensive numerical ocean models. A diffusion term could be added if smaller, molecular scales are also to be represented. In that case, our spectral results would still be valid for larger space and time scales.

There are also other stochastic models of turbulence that aim to capture the strong correlations observed in the ocean. These include the representation of joint particle motions through Langevin equations [12], which is hence capable of describing a complete flow. For the single particle, white noise in the Langevin equation can be replaced with fractional Gaussian noise to introduce stronger Eulerian correlations [13]. On the other hand, fractional Brownian motion can be used directly for a particle path in view of Lagrangian observations [14].

The paper is organized as follows. In Section 2, Çinlar velocity fields and flows are reviewed. In Section 3, we introduce the generalization of the decay parameter of the velocity field and show its consequences for a Kolmogorov spectrum. Finally, in Section 4, we derive the precise scaling of the parameters of the velocity field in the diffusive limit using the Markovian model and provide some simulation examples.

2 Homogeneous and Isotropic Çinlar Flows

In this section, we review flows generated by Çinlar velocity fields [1, 2, 3, 4, 5]. Let v be a deterministic velocity field on $\mathbb{R}^d$ called the *basic eddy*, and let $Q = \mathbb{R}^2 \times \mathbb{R} \times (0, \infty)$ be an index set. Eddies of different sizes and amplitudes for $q \in Q$, $x \in \mathbb{R}^d$ are obtained by

$$v_q(x) = a\, v(\frac{x-z}{b}) \qquad \text{for} \quad q = (z, a, b) \ . \tag{1}$$

Let N be a Poisson random measure on the Borel sets of $\mathbb{R} \times Q$ with mean measure

$$\mu(dt, dq) \equiv \mu(dt, dz, da, db) = \lambda \, dt \, dz \, \alpha(da)\beta(db) \tag{2}$$

where λ is the arrival rate per unit time-unit space, and α and β are probability distributions. The arrival time t of an eddy, its location z in space, its amplitude a as well as its scale b are all random and governed by N. By the superposition of these eddies appropriately decaying in time, a stationary velocity field u is constructed as

$$u(x,t) = \int_{(-\infty,t]\times Q} N(ds, dz, da, db) \, e^{-c(t-s)} \, a \, v(\frac{x-z}{b}) \qquad x \in \mathbb{R}^2, \ \ t \in \mathbb{R} \tag{3}$$

where $c > 0$ is the decay parameter [1]. The flow generated by u is defined as the family of solutions of the equation

$$\frac{d}{dt} X_t = u(X_t, t) \qquad X_0 = x \,, \qquad t \in \mathbb{R}_+ \,. \tag{4}$$

The stochastic construction of u as in (3) is motivated by the observation of eddies over the ocean surface, which seem to occur sporadically in time rather than continuously. A Poisson process captures arrivals that occur in this manner: independent from each other and one at a time. In view of this and with the aim of constructing a non-Gaussian velocity field, a Poisson random measure is used instead of a white noise that appears in the constructions based on stochastic differential equations such as a Brownian flow. We reserve the white noise as a diffusion term, which can be added to the right hand side of the flow equation (4). Hence, the velocity field (3) models larger scales than molecular. It is most appropriate for submesoscale eddies which are not usually resolved with the deterministic numerical models of the ocean at the mesoscale.

Çinlar velocity field has independent increments and hence is a Markov process. The exponential decay coefficient in (3) guarantees the Markovian property, which facilitates a more tractable analysis of the velocity field and its Lyapunov exponents. Nevertheless, the Markov velocity field u yields medium to long-term correlated particle paths consistent with Lagrangian observations of the ocean. A flow model based on a Markov velocity field such as u represents real oceanic flows more accurately than a Brownian flow. Markovian property holds for the resultant particle paths in a Brownian flow and indicate only short term correlation.

The velocity field is stationary, homogeneous and isotropic according to the following definitions. A velocity field u is said to be *stationary* (in the strict sense) if, for each $x \in \mathbb{R}^d$, the distribution of the collection $\{u(x, s+t) \, : \, t \in \mathbb{R}\}$ is the same for all $s \in \mathbb{R}$. A velocity field u is called *homogeneous* in space if, for each $t \in \mathbb{R}$, the probability law of the collection $\{u(z+x, t) \, : \, x \in \mathbb{R}^d\}$ is the same for all $z \in \mathbb{R}^d$. That is, the probability law of u_t is invariant under translations of the space $\mathbb{R}^d$. Isotropy corresponds to invariance of the same law under rotations and reflections of the coordinate system. Precisely, u is called *isotropic* if it is homogeneous and for each $t \in \mathbb{R}$ the probability laws of $\{u(Gx, t) \, : \, x \in \mathbb{R}^d\}$ and $\{G\, u(x, t) \, : \, x \in \mathbb{R}^d\}$ are the same for all orthogonal transformations G of $\mathbb{R}^d$. The verification of these properties [2] rely on the characteristic function formula

$$\mathbb{E} \exp i \int N(dx) f(x) = \exp \int \mu(dx)(e^{if(x)} - 1) \tag{5}$$

about integrals with respect to Poisson random measures [15] since the velocity field (3) is defined as such an integral. The finite dimensional distributions of u, that is, the distributions of

$$u(x_1, t_1), u(x_2, t_2), \ldots, u(x_n, t_n) \qquad x_1, \ldots, x_n \in \mathbb{R}^d, t_1, \ldots, t_n \in \mathbb{R}$$

determine the distribution of the collection $\{u(x, t) \; : \; x \in \mathbb{R}^d, t \in \mathbb{R}\}$. The characteristic function for such distributions is computed through the use of formula (5) and is given by

$$\begin{aligned} &\mathbb{E} \exp i \sum_{k=1}^{n} r_k \cdot u(x_k, t_k) = \\ &\quad \exp \int_{\mathbb{R}} \int_Q \mu(ds, dq)[\exp i \sum_{k=1}^{n} e^{-c(t_k - s)} r_k \cdot v_q(x_k) 1_{(-\infty, t_k]}(s) - 1] \end{aligned} \tag{6}$$

where dot denotes inner product and $r_1, \ldots, r_n \in \mathbb{R}^d$. Then, the mean measure (2) and the form (1) of the eddies are taken into account with $t_1 = \ldots = t_n = t$ where necessary, to verify the properties of stationarity, homogeneity and isotropy.

Since the flows considered in this paper are in $\mathbb{R}^2$, isotropy requires the basic eddy v to have a specific form. Namely, $v = (v^1, v^2)$ corresponds to rotation around 0 with magnitude $m(r)$ at distance r from 0, where $m : \mathbb{R} \to \mathbb{R}_+$ is continuous and has support $[0, 1]$. The specific equations for v are

$$v^1(x) = -\frac{x^2}{r}\, m(r) \qquad v^2(x) = \frac{x^1}{r}\, m(r) \tag{7}$$

where $x = (x^1, x^2)$ and $r = |x| \in [0, 1]$. As a rotation on $\mathbb{R}^2$, v is incompressible, that is, divergence free. We let it vanish outside the unit disk through the choice of m. Then, every eddy is a rotation, since it is translation, amplification and dilation of v. As a superposition of these *eddies*, the velocity field u is both incompressible and isotropic.

Several analytical and simulation results are available for Çinlar velocity fields. The Lyapunov exponents of the flow exist, and the top Lyapunov exponent appears to be strictly positive for the two dimensional incompressible flow [5]. As for simulation of flow and single particle dispersion, a range of ratios of two relevant time scales lead to a variety of particle paths [3]. Under some regimes, the paths are nearly Brownian, under other, the paths are clearly circular with some drift. Simulation with real ocean dimensions and homogenization through a diffusive term have been considered in addition to other physical aspects such as a Kolmogorov spectrum [8]. In homogeneous and incompressible flow, various dispersion measures are investigated for a mass cloud, single particle and a particle pair through simulation [4]. The relation of these measures with each other and the parameters of the velocity model is determined, and the physical predictions are confirmed.

3 Velocity Fields with Power-Law Spectra and Correlation Time

In this section, we formulate an important generalization of Çinlar velocity fields. In particular, we prove that a Kolmogorov type spectrum is achieved.

3.1 Generalization of Çinlar Velocity Fields

The main variation we introduce to the original Çinlar velocity field is the dependence of the decay parameter on the spatial variable x and the index q as

$$c_q(x) = c \left| \frac{x-z}{b} \right|^{2\gamma} \qquad \text{if} \quad q = (z, a, b) \tag{8}$$

for each $x \in \mathbb{R}^d$ where $c > 0$ as before and $\gamma > 0$. The decay rate is defined inversely proportional to the eddy scale b through a power-law in order to obtain a Kolmogorov type spectrum [9, 10] where γ controls the time correlation of the velocity field. Note that different decay rates are generated similar to different eddies. We will show that the particular form (8) is useful for representing the time and space dependence through separate parameters. The dependence of c_q on the spatial location relative to the center also identifies that an eddy may not retain the same shape as it decays.

For $x \in \mathbb{R}^2$, $t \in \mathbb{R}$, the velocity field is given by

$$u(x,t) = \int_{-\infty}^{t} \int_{Q} N(ds, dz, da, db)\, e^{-c|(x-z)/b|^{2\gamma}(t-s)}\, a\, v(\frac{x-z}{b}) \tag{9}$$

It can be proven as in [1, 2] that the velocity field (9) is stationary in time and homogeneous in space. Similarly, isotropy follows from the fact that the basic eddy v is a rotation. For the sake of clarity, we provide a proof of isotropy in the following theorem.

Theorem 1 *Let u be given by*

$$u(x,t) = \int_{-\infty}^{t} \int_{Q} N(ds, dz, da, db)\, e^{-c|(x-z)/b|^{2\gamma}(t-s)}\, a\, v(\frac{x-z}{b}) \qquad x \in \mathbb{R}^d, \quad t \in \mathbb{R}$$

where N is a Poisson random measure with mean measure

$$\mu(dt, dz, da, db) = \lambda\, dt\, dz\, \alpha(da)\beta(db)$$

on the Borel sets of $Q = \mathbb{R}^d \times \mathbb{R} \times (0, \infty)$. If the basic eddy v satisfies $v(Gx) = G\, v(x)$ for every orthogonal transformation G of $\mathbb{R}^d$, then u is isotropic.

Proof. We omit the proof of homogeneity which is necessary for isotropy. Fix an orthogonal transformation G of $\mathbb{R}^d$. We will show that the characteristic functions of $\{u(Gx,t) : x \in \mathbb{R}^d\}$ and $\{G\,u(x,t) : x \in \mathbb{R}^d\}$ are the same. We have

$$\begin{aligned}
&\int_Q dz\,\alpha(da)\beta(db)[\exp\, i\sum_{k=1}^n e^{-c|(Gx_k-z)/b|^{2\gamma}(t-s)}\, a\, r_k\cdot v(\frac{Gx_k-z}{b})-1]\\
&\quad=\int_Q dz\,\alpha(da)\beta(db)[\exp\, i\sum_{k=1}^n e^{-c|(Gx_k-Gz)/b|^{2\gamma}(t-s)}\, a\, r_k\cdot v(\frac{Gx_k-Gz}{b})-1]\\
&\quad=\int_Q dz\,\alpha(da)\beta(db)[\exp\, i\sum_{k=1}^n e^{-c|G\,\frac{x_k-z}{b}|^{2\gamma}(t-s)}\, a\, r_k\cdot v(G\frac{x_k-z}{b})-1]\\
&\quad=\int_Q dz\,\alpha(da)\beta(db)[\exp\, i\sum_{k=1}^n e^{-c|(x_k-z)/b|^{2\gamma}(t-s)}\, a\, r_k\cdot Gv(\frac{x_k-z}{b})-1]
\end{aligned}$$

where first equality follows from the invariance of the Lebesgue measure on $\mathbb{R}^d$ under orthogonal transformations G and third equality uses the hypothesis and the fact that $|Gx| = |x|$ for all $x \in \mathbb{R}^d$. Therefore, we get

$$\mathbb{E}\,\exp i\sum_{k=1}^n r_k\cdot u(Gx_k,t) = \mathbb{E}\,\exp i\sum_{k=1}^n r_k\cdot Gu(x_k,t)$$

in view of the characteristic function

$$\begin{aligned}
&\mathbb{E}\,\exp i\sum_{k=1}^n r_k\cdot u(x_k,t) =\\
&\qquad\exp\int_{-\infty}^t ds\int_Q dz\,\alpha(da)\beta(db)[\exp\, i\sum_{k=1}^n e^{-c|(x_k-z)/b|^{2\gamma}(t-s)}\, a\, r_k\cdot v(\frac{x_k-z}{b})-1]
\end{aligned}$$

which is similar to (6). As a result, the collections $\{u(Gx,t) : x \in \mathbb{R}^d\}$ and $\{G\,u(x,t) : x \in \mathbb{R}^d\}$ have the same distribution for each $t \in \mathbb{R}$. □

The covariance matrix R of the stationary and homogeneous velocity field u is given by

$$R_{ij}(x-y,|t-s|) = \mathbb{E}\,u_i(x,s)u_j(y,t)$$

as the mean velocity is zero due to isotropy. Let us compute R using the following formulas for expectations and variances of integrals with respect to Poisson random measures

$$\mathbb{E}\int N(dx)\,f(x) = \int \mu(dx)\,f(x)$$

and

$$\mathbb{E}\int \tilde{N}(dx)\int \tilde{N}(dx')\, f(x)\, g(x') = \int \mu(dx)\, f(x)\, g(x)$$

where $\tilde{N}(dx) = N(dx) - \mu(dx)$. Then, for $x, y \in \mathbb{R}^2$ and $s, t \in \mathbb{R}$, $s < t$ without loss of generality, $i, j = 1, 2$, we have

$$\begin{aligned}
&R_{ij}(x-y, |t-s|) \\
&= \mathbb{E}\int_{-\infty}^{s}\int_{Q}\tilde{N}(dr,dq)\, e^{-c_q(x)(s-r)}\, v_q^i(x)\int_{-\infty}^{s}\int_{Q}\tilde{N}(dr,dq)\, e^{-c_q(y)(t-r)}\, v_q^j(y) \\
&= \lambda\int_{-\infty}^{s} dr\int_{Q} dz\, \alpha(da)\beta(db)\, e^{-c_q(x)(s-r)}e^{-c_q(y)(t-r)}v_q^i(x)v_q^j(y) \\
&= \lambda\int_{Q} dz\, \alpha(da)\beta(db)\,\frac{e^{-c|(y-z)/b|^{2\gamma}(t-s)}}{c|(x-z)/b|^{2\gamma}+c|(y-z)/b|^{2\gamma}}\, av_i(\frac{x-z}{b})\, av_j(\frac{y-z}{b}) \\
&= \lambda\int_{\mathbb{R}^2} dz\int_{\mathbb{R}}\alpha(da)\int_{\mathbb{R}_+}\beta(db)\,\frac{a^2b^2\, e^{-c|z|^{2\gamma}|t-s|}}{c|z|^{2\gamma}+c|z+(x-y)/b|^{2\gamma}}v_i(z)v_j(z+\frac{x-y}{b})
\end{aligned}$$

where the last line is obtained through a change of variable $(y-z)/b$ to z.

For a power-law decay of covariances in the spatial variable, we choose the distribution β of b as a power-law distribution. An example is a Pareto distribution with the probability density function $f(b) = \delta l_1^{\delta} b^{-\delta-1}$, $b \geq l_1$, where $\delta > 0$ is a shape parameter and $l_1 > 0$ is a scale parameter that serves as the ultraviolet cutoff scale for the spectrum. In order to generate various power-law scalings in the inertial range and have finite energy, we instead use an evolutionary Pareto, also called biPareto, distribution [22] given by

$$\beta(db) = \begin{cases} \delta l_1^{\delta} b^{-\delta-1}\, db & \text{if } \; l_1 \leq b < l_2 \\ \theta l_1^{\delta} l_2^{\theta-\delta} b^{-\theta-1}\, db & \text{if } \; b \geq l_2 \end{cases} \tag{10}$$

where $\delta, \theta > 0$ are the parameters to capture power-law dependence, and $l_1, l_2 > 0$ will serve as the cutoff scales. Note that the distribution in (10) has a piecewise continuous density function with a discontinuity at l_2, while it satisfies $\int_{l_1}^{\infty}\beta(db) = 1$. Hence, we have

$$R_{ij}(x,t) = \tag{11}$$
$$\frac{\lambda\delta l_1^{\delta}}{c}\int_{\mathbb{R}}\alpha(da)\, a^2\int_{\mathbb{R}^2} dz\, e^{-c|z|^{2\gamma}|t|}\int_{l_1}^{l_2} db\, b^{1-\delta}\frac{1}{|z|^{2\gamma}+|z+x/b|^{2\gamma}}\, v_i(z)v_j(z+\frac{x}{b})$$

$$+\frac{\lambda\theta l_1^{\delta} l_2^{\theta-\delta}}{c}\int_{\mathbb{R}}\alpha(da)\,a^2\int_{\mathbb{R}^2}dz\,e^{-c|z|^{2\gamma}|t|}\int_{l_2}^{\infty}db\,b^{1-\theta}\frac{1}{|z|^{2\gamma}+|z+x/b|^{2\gamma}}\,v_i(z)v_j(z+\frac{x}{b})$$

for $x\in\mathbb{R}^d$ and $t\in\mathbb{R}$.

3.2 Spatial Long-Range Correlation

A stationary process X_t with autocorrelation function ρ is said to have long-range correlations if there exists $0<\alpha<1$ and $c_\rho>0$ such that $\lim_{x\to\infty}\rho(x)/(c_\rho x^{-\alpha})=1$ [16]. For stationary and homogeneous velocity fields, long-range correlation is considered for the spatial variable only [9, 17]. On the other hand, temporal correlation obtained from Lagrangian measurements agree well with an exponential form as in (11).

We study $R_{11}(x,0)+R_{22}(x,0)$, which is a function of $|x|$ due to isotropy, as $|x|\to\infty$. Putting (7) in (11) and using the identity

$$z^1(z^1+\frac{x^1}{b})+z^2(z^2+\frac{x^2}{b})=\frac{(|z+x/b|^2+|z|^2-|x|^2/b^2)}{2}$$

we get

$$\begin{aligned}&R_{11}(x,0)+R_{22}(x,0)\\&\quad=\frac{\lambda\delta l_1^{\delta}\mathbb{E}a^2}{c}\int_{\mathbb{R}^2}dz\int_{l_1}^{l_2}db\,b^{1-\delta}\frac{(|z+x/b|^2+|z|^2-|x|^2/b^2)\,m(|z|)\,m(|z+x/b|)}{2|z||z+x/b|(|z|^{2\gamma}+|z+x/b|^{2\gamma})}\\&\qquad+\frac{\lambda\theta l_1^{\delta} l_2^{\theta-\delta}\mathbb{E}a^2}{c}\int_{\mathbb{R}^2}dz\int_{l_2}^{\infty}db\,b^{1-\theta}\frac{(|z+x/b|^2+|z|^2-|x|^2/b^2)\,m(|z|)\,m(|z+x/b|)}{2|z||z+x/b|(|z|^{2\gamma}+|z+x/b|^{2\gamma})}\end{aligned}$$

By making a change of variable $b/|x|$ to b, we obtain

$$\begin{aligned}&R_{11}(x,0)+R_{22}(x,0)\\&\quad=\frac{\lambda\delta l_1^{\delta}\mathbb{E}a^2}{2c}|x|^{2-\delta}\int_{l_1/|x|}^{l_2/|x|}db\,b^{1-\delta}\int_{\mathbb{R}^2}dz\,\frac{(|z+\frac{x}{|x|b}|^2+|z|^2-\frac{1}{b^2})\,m(|z|)\,m(|z+\frac{x}{|x|b}|)}{|z||z+\frac{x}{|x|b}|(|z|^{2\gamma}+|z+\frac{x}{|x|b}|^{2\gamma})}\\&\qquad+\frac{\lambda\theta l_1^{\delta} l_2^{\theta-\delta}\mathbb{E}a^2}{2c}|x|^{2-\theta}\int_{l_2/|x|}^{\infty}db\,b^{1-\theta}\int_{\mathbb{R}^2}dz\,\frac{(|z+\frac{x}{|x|b}|^2+|z|^2-\frac{1}{b^2})\,m(|z|)\,m(|z+\frac{x}{|x|b}|)}{|z||z+\frac{x}{|x|b}|(|z|^{2\gamma}+|z+\frac{x}{|x|b}|^{2\gamma})}\end{aligned}\tag{12}$$

Now, recall that m has a compact support, namely [0,1]. The model spans a wide spectrum of eddy scales only through b. As a result, for each fixed x, the innermost integral on $\mathbb{R}^2$ above is effectively on $A = \{z : |z + e_x/b| \le 1, |z| \le 1, e_x \in \mathbb{R}^2, z \in \mathbb{R}^2\}$ where e_x is the unit vector $x/|x|$. For $|x|$ sufficiently large, $l_2/|x| \le 1/2$ and for values of b less than $1/2$, the set A is empty. Hence, the integral on b is effectively on a subset of $[1/2, \infty)$ in the second summand in (12), independent of x for large $|x|$. We fix the direction of x and let $|x|$ grow without loss of generality due to isotropy. It follows that

$$\lim_{|x|\to\infty} \frac{R_{11}(x,0) + R_{22}(x,0)}{|x|^{2-\theta}} = C$$

for a constant $C > 0$. Therefore, u has long-range correlations in space with $\theta - 2$ for α in the definition, when $2 < \theta < 3$. Its Hurst parameter is given by [16]

$$H = \frac{4-\theta}{2} \qquad \frac{1}{2} < H < 1\,.$$

Of course, the choice of particular m depends on γ so that the covariance R is finite.

Çinlar velocity fields as given in Section 2 model medium scale structures which Brownian flows cannot capture. They can also have long-range correlation as long as we pick the distribution β as in (10) representing almost all scales from small to large. Spatial correlation in long-range correlated Ornstein-Uhlenbeck flows [17] is governed by a single parameter similar to δ or θ here. Another parameter, here γ, controls the temporal correlation for Kolmogorov spectrum, which will be discussed next.

Remark. We could have chosen the decay parameter as $c/b^{2\gamma}$ with $c > 0$ instead of $c_q(x)$ of (8). However, the spatial covariance would be governed by both θ and γ in that case and there would not be separate parameters for the time and space dependence. Namely, $R_{11}(x,0) + R_{22}(x,0)$ would be proportional to $|x|^{2-\theta+2\gamma}$ for large x.

3.3 Kolmogorov Spectrum

The Fourier transform E of R is called the *spectral density tensor* given by

$$E_{ij}(k,w) = \frac{1}{(2\pi)^d} \int_{\mathbb{R}} \int_{\mathbb{R}^d} \mathrm{e}^{-i(k\cdot x + wt)} R_{ij}(x,t)\, dx\, dt \qquad i,j = 1,\ldots,d\,.$$

Energy spectrum $\mathcal{E}$ is obtained from E by removing all directional information. It is defined as

$$\mathcal{E}(|k|) = \frac{1}{2} \sum_{i=1}^{d} \oint \int_{\mathbb{R}} E_{ii}(k, w)\, dw\, dS(|k|) \tag{13}$$

where $S(|k|)$ is the sphere in wavenumber space, centered at the origin, with radius $|k|$, and $\oint dS(|k|)$ denotes integration over this surface [11, 18]. If the velocity field has no time dependence, $\mathcal{E}$ completely determines E in isotropic turbulence.

For Ornstein-Uhlenbeck velocity fields with Kolmogorov type spectra [9], the spectral density is constructed for $k \in \mathbb{R}^d$, $w \in \mathbb{R}$ as

$$E_{ij}(k, w) = \frac{\beta(k)}{w^2 + \beta(|k|)^2} \frac{\mathcal{E}(|k|)}{|k|^{d-1}} \left(\delta_{ij} - \frac{k_i k_j}{|k|^2} \right)$$

where δ_{ij} is Kronecker delta and the energy spectrum $\mathcal{E}$ is usually chosen to be zero near the origin and near infinity, and to behave like a power in the inertial range. This power behavior controls the spatial correlation, whereas β usually chosen also as a power form controls the time correlation. For the same type velocity fields, a covariance matrix of the following form is also considered [17, 19, 20]

$$R_{ij}(x, t) = \int_{\mathbb{R}^d} e^{-|k|^{2\beta} t} \cos(k \cdot x) \frac{\mathcal{E}(|k|)}{|k|^{d-1}} \left(\delta_{ij} - \frac{k_i k_j}{|k|^2} \right) dk \tag{14}$$

where $\beta > 0$, $t > 0$, $x \in \mathbb{R}^d$, and $\mathcal{E}$ is the energy spectrum given by $\mathcal{E}(r) = a(r) r^{1-2\alpha}$, $r > 0$ for $\alpha > 0$ and a proper ultraviolet or infrared cutoff function a.

The energy spectrum for Çinlar velocity fields for $d = 2$ is given by [8]

$$\mathcal{E}(|k|) = \frac{\pi^3}{c} |k| \int_{\mathbb{R}} \alpha(da) a^2 \int_{\mathbb{R}_+} \beta(db) b^4 \hat{v}(bk) \cdot \hat{v}(-bk)$$

where $k \in \mathbb{R}^2$ and $\hat{v}$ is the Fourier transform of the basic eddy v, that is,

$$\hat{v}(k) = \frac{1}{(2\pi)^d} \int_{\mathbb{R}^d} e^{-ik \cdot x} v(x)\, dx \; .$$

The proof of this result uses the fact that turbulent energy per unit mass is defined in physical space as $(1/2) \sum_{i=1}^{d} R_{ii}(0, 0)$, which is equivalent to

$$\frac{1}{2} \int_{\mathbb{R}^d} \sum_{i=1}^{d} \frac{1}{(2\pi)^d} \int_{\mathbb{R}^d} e^{-ik \cdot x} R_{ii}(x, 0)\, dx\, dk =: \int_0^\infty \mathcal{E}(|k|)\, d|k| \; . \tag{15}$$

This definition of $\mathcal{E}$ is consistent with (13). We follow the same lines of the proof in [8] using (11) for the velocity field (9). By rearranging the integrals and making a change of variable $z + x/b$ to x, we get

$$\begin{aligned}
&\int_{\mathbb{R}^d} e^{-ik\cdot x} R_{ij}(x,0)\, dx \\
&\quad = \frac{\lambda\delta l_1^\delta \mathbb{E}a^2}{c} \int_{l_1}^{l_2} db\, b^{3-\delta} \int_{\mathbb{R}^2} dz\, e^{ibk\cdot z} v_i(z) \int_{\mathbb{R}^2} dx\, e^{-ibk\cdot x} \frac{v_j(x)}{|z|^{2\gamma} + |x|^{2\gamma}} \\
&\quad\quad + \frac{\lambda\theta l_1^\delta l_2^{\theta-\delta} \mathbb{E}a^2}{c} \int_{l_2}^{\infty} db\, b^{3-\theta} \int_{\mathbb{R}^2} dz\, e^{ibk\cdot z} v_i(z) \int_{\mathbb{R}^2} dx\, e^{-ibk\cdot x} \frac{v_j(x)}{|z|^{2\gamma} + |x|^{2\gamma}}\,.
\end{aligned}$$

It can be shown as in [7, Proposition II.2.12] that $\sum_{i=1}^2 \int_{\mathbb{R}^d} e^{-ik\cdot x} R_{ii}(x,0)\, dx$ depends on k only through $|k|$. Hence, letting

$$f(b|k|) := \sum_{i=1}^{2} \int_{\mathbb{R}^2} dz\, e^{ibk\cdot z} v_i(z) \int_{\mathbb{R}^2} dx\, e^{-ibk\cdot x} \frac{v_j(x)}{|z|^{2\gamma} + |x|^{2\gamma}}\,,$$

making a change of variable $b|k|$ to b, putting in (15), and changing the integral in k to polar coordinates, we get

$$\begin{aligned}
\mathcal{E}(|k|) &= \frac{2\pi|k|}{2(2\pi)^2} \left(\frac{\lambda\delta l_1^\delta \mathbb{E}a^2}{c} \int_{|k|l_1}^{|k|l_2} db\, \frac{b^{3-\delta}}{|k|^{4-\delta}} f(b) + \frac{\lambda\theta l_1^\delta l_2^{\theta-\delta} \mathbb{E}a^2}{c} \int_{|k|l_2}^{\infty} db\, \frac{b^{3-\theta}}{|k|^{4-\theta}} f(b) \right) \\
&= \frac{\lambda\delta l_1^\delta \mathbb{E}a^2}{4\pi c} |k|^{\delta-3} \int_{|k|l_1}^{|k|l_2} db\, b^{3-\delta} f(b) + \frac{\lambda\theta l_1^\delta l_2^{\theta-\delta} \mathbb{E}a^2}{4\pi c} |k|^{\theta-3} \int_{|k|l_2}^{\infty} db\, b^{3-\theta} f(b)\,. \qquad (16)
\end{aligned}$$

By similar arguments of Section 3.2, the second integral in (16) does not depend on $|k|$ for small $|k|$. Hence, we must have $\theta > 2$ for finite energy. The velocity field is said to be long-range correlated also if $\theta < 3$, which is consistent with the results of Section 3.2 in view of [15, Theorem 2.1].

The interval (l_1, l_2), $l_1, l_2 \in \mathbb{R}_+$, corresponds to the inertial scales. In particular, Kolmogorov's spectrum for the inertial range can be obtained with $\delta = 4/3$, since then, $\mathcal{E}(|k|) \sim |k|^{-5/3}$ in (16). If modeling goes through only the spectral density tensor, then confining to the inertial range wavenumbers is adequate [10]. By means of θ, we generate a complete spectrum including the inertial range as well as the energy containing larger scales, equivalently, smaller wavenumbers. For $|k|^2$ or $|k|^4$ behavior of $\mathcal{E}$ at the origin [18, 21], θ must take values 5 or 7, respectively. In view of (12), the values 5 or 7 for θ indicate that R decays rapidly as $|x|^{-3}$ or $|x|^{-5}$, respectively, as $|x| \to \infty$. When $l_1 < |x| < l_2$, namely $|x|$ is in the inertial scales, the first term dominates. At the dissipation scales $(0, l_1)$, the structure function, which is $4[R(0,0) - R(x,0)]$, grows as $|x|^2$. This follows from Taylor expansion as R is an even function in x provided that it is twice continuously differentiable. This amounts to assuming that the magnitude function m is twice differentiable everywhere.

The velocity field (9) being Markovian in time has an exponential autocorrelation, but with an extra parameter γ that will be handy in replicating Kolmogorov spectrum for fully developed turbulence in three dimensions. The ocean surface is an interface of a three dimensional field and does not necessarily obey two dimensional fluid dynamics laws [8]. On scales smaller than the vertical layering depth, it exhibits aspects of three dimensional turbulence. That is why, we will choose $\delta = 4/3$ in the inertial range to reproduce Kolmogorov's $-5/3$ spectrum. This is consistent with 2/3 law [21] for the second order structure function given by $\mathbb{E}|u(y + x, t) - u(x, t)|^2$ which is equal to $4\sum_{i=1}^{2}[R_{ii}(0, 0) - R_{ii}(x, 0)]$. Indeed, we can show similar to the derivation of (12) that

$$\sum_{i=1}^{2}[R_{ii}(0,0) - R_{ii}(x,0)] = \frac{\lambda\delta l_1^{\delta}\mathbb{E}a^2}{2c}|x|^{2-\delta}\int_{l_1/|x|}^{l_2/|x|} db\, b^{1-\delta}\int_{\mathbb{R}^2} dz \cdot \left[\frac{m^2(|z|)}{2|z|^{2\gamma}} - \frac{(|z + \frac{x}{|x|b}|^2 + |z|^2 - \frac{1}{b^2})\, m(|z|)\, m(|z + \frac{x}{|x|b}|)}{2|z||z + \frac{x}{|x|b}|(|z|^{2\gamma} + |z + \frac{x}{|x|b}|^{2\gamma})}\right] + \phi(\theta)$$

which is proportional to $|x|^{2/3}$ with $\delta = 4/3$ for $|x|$ sufficiently greater than l_1, in the inertial range. Here, we have omitted the terms that depend on parameter θ and denoted simply by $\phi(\theta)$.

Note that the time correlation parameter γ is similar to β of Equation (14) which is chosen to be 1/3 for Kolmogorov scaling [10]. For determining γ, we consider b as a length scale of the model. We aim to obtain a time scale in terms of b to relate to Kolmogorov spectrum. A simple approach would be using the reciprocal of the decay rate $1/c_q$ as a time scale which is proportional to $b^{2\gamma}/c$ omitting the dependence on $|x-z|$. Note that if we had the simpler version $c_q = c/b^{2\gamma}$, then the time scale would be simply equal to $b^{2\gamma}/c$.

Alternatively, we can consider Eulerian correlation time as a time scale of the model given by [3]

$$\tau_E = \frac{1}{2\pi}\int_{\mathbb{R}} [R_{11}(0,t) + R_{22}(0,t)]\, dt \;/\; [R_{11}(0,0) + R_{22}(0,0)] \tag{17}$$

We indicate only the relevant, namely, inertial scales in the following derivation for the sake of clarity and denote the remaining term as $\Phi(\theta)$. From (11) and (7), the numerator of (17) is

$$\begin{aligned} &\frac{1}{2\pi}\int_{\mathbb{R}} [R_{11}(0,t) + R_{22}(0,t)]\, dt \\ &\quad = \frac{1}{2\pi}\frac{\lambda\delta l_1^{\delta}\mathbb{E}a^2}{c}\int_{\mathbb{R}} dt \int_{l_1}^{l_2} db\, b^{1-\delta}\int_{\mathbb{R}^2} dz\, e^{-c|z|^{2\gamma}|t|}\frac{1}{2|z|^{2\gamma}}\, m^2(|z|) + \Phi(\theta) \\ &\quad = \frac{\lambda\delta l_1^{\delta}\mathbb{E}a^2}{2\pi c}\int_{\mathbb{R}^2} dz\, |z|^{-\delta}\int_{l_1/|z|}^{l_2/|z|} db\, b^{2\gamma-\delta-1}\, m^2(1/b)\int_0^{\infty} dt\, e^{-ct/b^{2\gamma}} + \Phi(\theta) \end{aligned} \tag{18}$$

found by making change of variables bz to z for z variable, then $b/|z|$ to b for b variable which suppresses the dependence on z of the innermost integral. The denominator of (17) scales the quantity in (18) to obtain the units of time. However, the integral $\int_0^{\infty} dt\, e^{-ct/b^{2\gamma}}$ is the crucial term for obtaining a time scale as it is an integral over time. Therefore, we define the time scale T at the spatial scale b to be

$$T = \int_0^{\infty} dt\, e^{-ct/b^{2\gamma}} = \frac{b^{2\gamma}}{c} \tag{19}$$

which is the same as the time scale defined in terms of the decay rate above. Eulerian correlation time τ_E has a power-law dependence on spatial scale b, locally.

We consider b as the length scale L at wavenumbers k with $|k| \sim 1/b$. Kolmogorov's scaling law in the inertial range is

$$\mathcal{E}(|k|) = C\varepsilon^{2/3}|k|^{-5/3} \tag{20}$$

where C is a dimensionless constant. Considering (20) with the dimensions of the energy spectrum $\mathcal{E}$ and the mean dissipation rate ε, which are L^3/T^2 and L^2/T^3, respectively, we get

$T \propto \varepsilon^{-1/3} b^{2/3}$. In view of (19), we can choose

$$c = \varepsilon^{1/3} \ , \qquad \gamma = 1/3 \ ,$$

C as a constant related to those in (16), as well as $\delta = 4/3$.

We plot the empirical power spectral density function versus frequency in Figure 1, using $\gamma = 1/3$ and $\delta = 4/3$. The density is obtained by partitioning the spatial grid of a single run in view of homogeneity. Only one of the formerly studied set of parameters [3], except for the obvious difference in the decay parameter and the distribution of the radius b introduced in the present paper, is given here for illustration of 5/3 scaling. This set of parameters yields a mixture of irregular and circular paths in contrast to diffusive paths that will be discussed in Section 4. The others corresponding to different regimes of motion [3] also yield the same 5/3 scaling as expected, when γ and δ are selected as above. In the simulation, b can take at most the value l_2 which serves as an infrared cutoff and hence θ is not used.

To replicate Kolmogorov scaling for the original Çinlar velocity field (3), a joint distribution for a and b is considered as [8]

$$\kappa(da, db) = C(r, q) \int_{-L}^{L} dx\, \delta_{xb^q}(da) b^r\, db \qquad b \in (b_1, b_2) \tag{21}$$

where $L, b_1, b_2 > 0$, δ_x is the Dirac measure sitting at x, $r, q > 0$ are parameters and $C(r, q)$ is a normalizing constant that depend on them. That is, the mean measure (2) is taken to be $\mu(dt, dz, da, db) = \lambda dt\, dz\, \kappa(da, db)$ which characterizes the distribution of the Poisson random measure N through the characteristic function given in (5). In this setting, a can be considered as the typical velocity in order to connect its distribution to the dissipation rate ε. In the present study, the decay rate c plays this role.

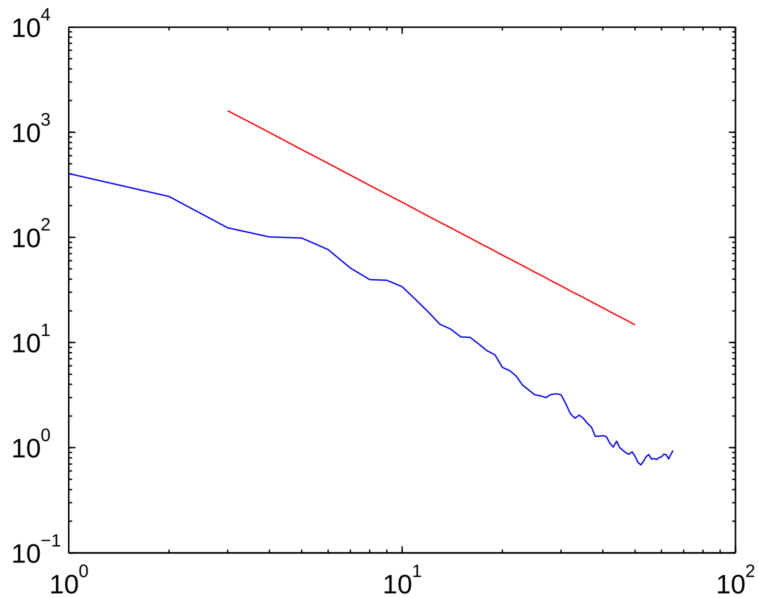

Figure 1: Log-log plot of power spectral density versus frequency. The straight line has slope -5/3, $c = 0.1, \lambda = 0.1, a \sim$ Unif(-5.4,5.4), $(l_1, l_2) = (0.1, 2)$

4 Diffusive Limit

In this section, we consider the Markovian velocity field

$$u(x,t) = \int_{(-\infty,t]\times Q} N(ds, dz, da, db)\, e^{-c(t-s)}\, a\, v(\frac{x-z}{b}) \qquad x \in \mathbb{R}^2,\ t \in \mathbb{R} \tag{22}$$

given earlier in Equation (3). This corresponds to the velocity field (9) having $\gamma = 0$. With a mean measure that involves (21), it satisfies Kolmogorov spectrum as well as being Markovian [8]. Using previous results on Markovian velocity fields, we show that the single particle path generated by the velocity field (22) becomes a diffusion in the limit with a proper scaling in time and space. The scaling for the particle path corresponds to the scaling of the parameters of the velocity field in time and space explicitly whereas for Ornstein-Uhlenbeck velocity fields the scaling is in the frequency domain. Hence, our results further provide an understanding of the dynamics for a diffusion limit.

The single particle path in a flow based on the velocity field u is the solution of the ordinary differential equation

$$\frac{d}{dt} X_t = u(X_t, t) \qquad X_0 = x \ , \quad t \in \mathbb{R}_+ \tag{23}$$

For velocity fields that are Markovian, stationary, homogeneous and incompressible, it has been shown in [23] that the single particle path scaled with $\epsilon > 0$, given by

$$X_t^\epsilon = \epsilon X_{t/\epsilon^2} \qquad t \geq 0 \tag{24}$$

converges to a Brownian motion as $\epsilon \to 0$, provided that the velocity field satisfies a spectral gap condition. An example is the stationary and divergence-free Ornstein-Uhlenbeck velocity field with a corresponding condition on its spectral measure. It has been shown in [5] that the velocity field u satisfies such a spectral gap. Namely, there exists a constant $k > 0$ such that

$$-(LF, F)_{L^2(E,\zeta)} \geq k \, \|F\|^2_{L^2(E,\zeta)}$$

for all F in the domain of L with $\int_E \zeta(dy) \, F(y) = 0$ where L is the generator of the Markovian velocity field u. Hence, the scaled path X^ϵ on u converges to a Brownian motion when u is of the form (22). The proof of this result [5] does not depend on the form of the joint distribution of a and b. Therefore, the single particle path X^ϵ converges to a diffusion in the limit, also when it is generated through the distribution (21).

It follows from Equation (23) that (24) is equivalent to the following scaling of the velocity field

$$u^\epsilon(x,t) = \frac{1}{\epsilon} \, u\left(\frac{x}{\epsilon}, \frac{t}{\epsilon^2}\right) \qquad x \in \mathbb{R}^d, \ t \in \mathbb{R}_+ \ .$$

That is, X^ϵ is the solution to (23) with the velocity field u^ϵ. Scrutinizing this scaling of the velocity field, we can show that the diffusion limit is obtained when the eddies arrive fast, decay fast, and rotate fast with a small radius. This is quite intuitive in view of the emergence of central limit theorem in various applications.

With the non-Markovian velocity field (9), diffusion limits can be sought only with techniques other than Markov property of the Lagrangian velocity. In particular, Markovian non-mixing or Ornstein-Uhlenbeck flows have been studied for diffusive and non-diffusive limits [17, 19, 20]. What is referred as a non-diffusive limit here is a fractional Brownian motion (FBM). Drifter observations indicate that the flow in the ocean is much more correlated in time than a Brownian motion. As a result, an FBM is sometimes used for modeling transport [14]. A persistent FBM is a Gaussian process with Hurst parameter $H \in (1/2, 1)$ and reduces to ordinary Brownian motion for $H = 1/2$. Its increment process called fractional Gaussian noise is stationary with long-range correlations if $H > 1/2$. We intend to investigate the possibility of an FBM limit for the particle motion as future work. Lamperti's theorem [24] suggests that $X_t^\epsilon = \epsilon X_{t/\epsilon^{1/H}}$ could be a candidate scaling of the particle motion X. For $H = 1/2$, this reduces to the same scaling as (24) which yields an ordinary Brownian motion as expected. For Ornstein-Uhlenbeck flows, the large scale limit is a Brownian motion in presence of an infrared cutoff which is required for finite energy. If the infrared cutoff is gradually removed as $\epsilon \to 0$, then the limit is still a Brownian motion [25]. Therefore, our search for an FBM limit requires further analysis.

5 Conclusions

In this paper, we have considered a generalization of homogeneous and isotropic Çinlar velocity fields to model power-law correlation across spatial scales. This has been achieved by making the decay rate depend on essentially the eddy radius which is assumed to have a power-law distribution. Long-range correlation in space is also studied and a similar spectrum previously used with Ornstein-Uhlenbeck velocity fields is replicated. Such models are constructed with assumptions on the spectra, whereas our model originates from observed structures of eddies and randomness in the ocean. We have obtained the spectral properties as a consequence of the choice of the parameters and the probability distributions. The parameters of the probability distributions are further specified in view of Kolmogorov theory of the inertial scales. In particular, $|k|^{-5/3}$ scaling of the spectrum is obtained.

We have used an exponential form for temporal correlation for replicating the covariance used earlier with Ornstein-Uhlenbeck flows. On the other hand, one can construct various stationary and homogeneous velocity fields by

$$\int_{-\infty}^{t} \int_{Q} N(ds, dq)\, f(t-s, x-z, a, b)\, v_q(x)$$

where $f : \mathbb{R}_+ \times \mathbb{R}^d \times \mathbb{R} \times \mathbb{R}_+ \to \mathbb{R}$ is such that the velocity field is square integrable. As for future work, the form of f and the distribution of a can be selected so that u has a different correlation structure in time motivated by Eulerian observations.

Finally, we have shown that the single particle trajectory of the original Markovian velocity field converges to a Brownian motion with a proper scaling in time and space. For the generalized velocity field which is no more Markovian, any diffusive or non diffusive limits are left as future work.

Acknowledgements

The author would like to thank anonymous referees for their constructive comments that significantly improved this work.

References

[1] Çinlar, E. On a Random Velocity Field. Princeton University (1993).

[2] Çinlar, E. Isotropic Velocity Fields of Poisson Shot Noise Type. Princeton University (1994).

[3] M. Çağlar, Simulation of homogeneous and incompressible Çinlar flows, *Appl. Math. Modelling*, **24** (2000) 297-314.

[4] M. Çağlar, Dispersion of mass by two-dimensional homogeneous and incompressible Çinlar flows, *Appl. Math. Modelling* **27** (2003) 997-1011.

[5] M. Çağlar and E. Çinlar Lyapunov Exponents of Poisson Shot-Noise Velocity Fields, *Stochastic Processes and their Applications*, **94** (2001) 29-49.

[6] L.K. Shay et al., VHF radar detects oceanic submesoscale vortex along Florida coast, *Eos Trans.*, **81** (2000) 209-213.

[7] M. Çağlar, T. Ozgokmen, L.I. Piterbarg, Parameterization of submeso-scale eddy-rich flows using a stochastic velocity model, *Journal of Atmospheric and Oceanic Technology*, to appear (2006).

[8] H.E. Yildirim, Poisson random velocity fields: advection-diffusion properties. Dissertation, Princeton University (1998).

[9] R. A. Carmona Transport properties of Gaussian velocity fields, in Real and Stochastic Analysis: Recent Advances ed. M.M. Rao CRC Press, (1997) 9-63.

[10] A. Fannjiang, Invariance principle for inertial-scale behavior of scalar fields in Kolmogorov-type turbulence, *Physica D* **179** (2003) 161-182.

[11] A. J. Majda and P. K. Kramer, Simplified models for turbulent diffusion: Theory, numerical modelling, and physical phenomena, *Physics Reports* **314** (1999) 237-574.

[12] L.I. Piterbarg, The top Lyapunov exponent for a stochastic flow modeling the upper ocean turbulence. SIAM J.Appl. Math, **62** (2001) 777-800.

[13] Y. Shao, The fractional Ornstein-Uhlenbeck process as a representation of homogeneous Eulerian velocity turbulence, *Physica D* **83** (1995) 461-477.

[14] P.S. Addison, A method for Modelling Dispersion Dynamics in Coastal Waters Using Fractional Brownian Motion, *Journal of Hydraulic Research*, **34** (1996) 549-561.

[15] O. Kallenberg, *Random Measures* (Academic Press, 1983).

[16] J. Beran, *Statistics of Long Memory Processes* (Chapman & Hall, 1994).

[17] A. Fannjiang and T. Komorowski, Diffusions in long-range correlated Ornstein-Uhlenbeck flows, *Elect. Journ. of Prob.* **7** (2002) 1-22.

[18] S.B. Pope, *Turbulent Flows* (Cambridge University Press, 2000).

[19] A. Fannjiang and T. Komorowski, Fractional Brownian motions in a limit of turbulent transport, *Annals of Applied Probability* **10** (2000) 1100-1120.

[20] A. Fannjiang and T. Komorowski, Diffusive and nondiffusive limits of transport in nonmixing flows, *SIAM Journal on Appl. Math.* **62:** (2002) 909-923.

[21] J. Mathieu and J. Scott, *An Introduction to Turbulent Flow* (Cambridge University Press, 2000).

[22] D. Picard and K. Tribouley, Evolutionary Pareto Distributions, *Ann. I. H. Poincaré* - PR **38** (2002) 1023-1037.

[23] A. Fannjiang and T. Komorowski, Turbulent Diffusion in Markovian Flows, *Annals of Applied Probability* **9** (1999) 591-610.

[24] W. Vervaat, Properties of general self-similar processes, *Bull. Internat. Statis. Inst.*, **52** (1987) (4): 199-216.

[25] A. Fannjiang, Phase Diagram for Turbulent Transport: Sampling Drift, Eddy Diffusivity and Variational Principles, *Physica D* **136** (2000): 145-174.

Abbreviated Title

Velocity Fields with Power-Law Spectra

Figure Captions

Figure 1. Log-log plot of power spectral density versus frequency. The straight line has slope -5/3, $c = 0.1, \lambda = 0.1, a \sim$ Unif(-5.4,5.4), $(l_1, l_2) = (0.1, 2)$